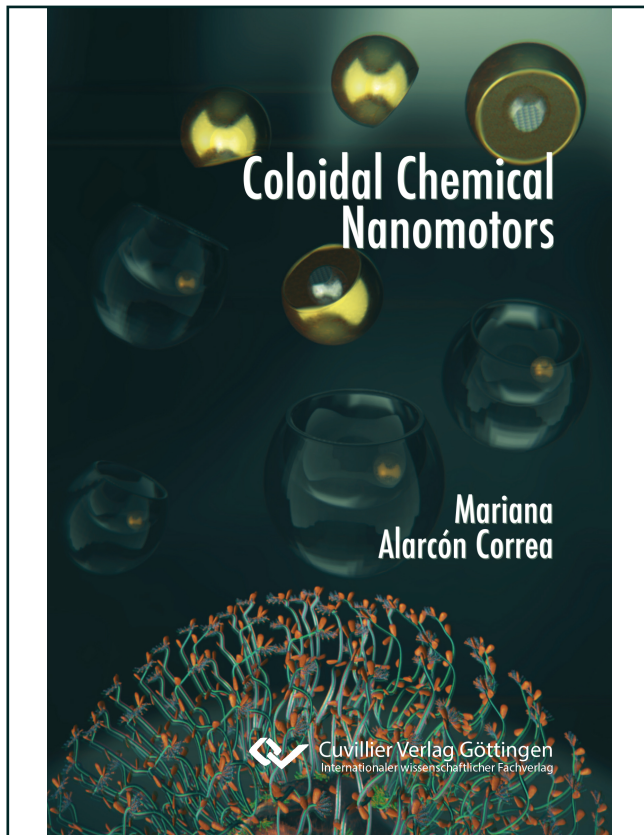




Mariana Alarcón Correa (Autor)  
**Colloidal Chemical Nanomotors**

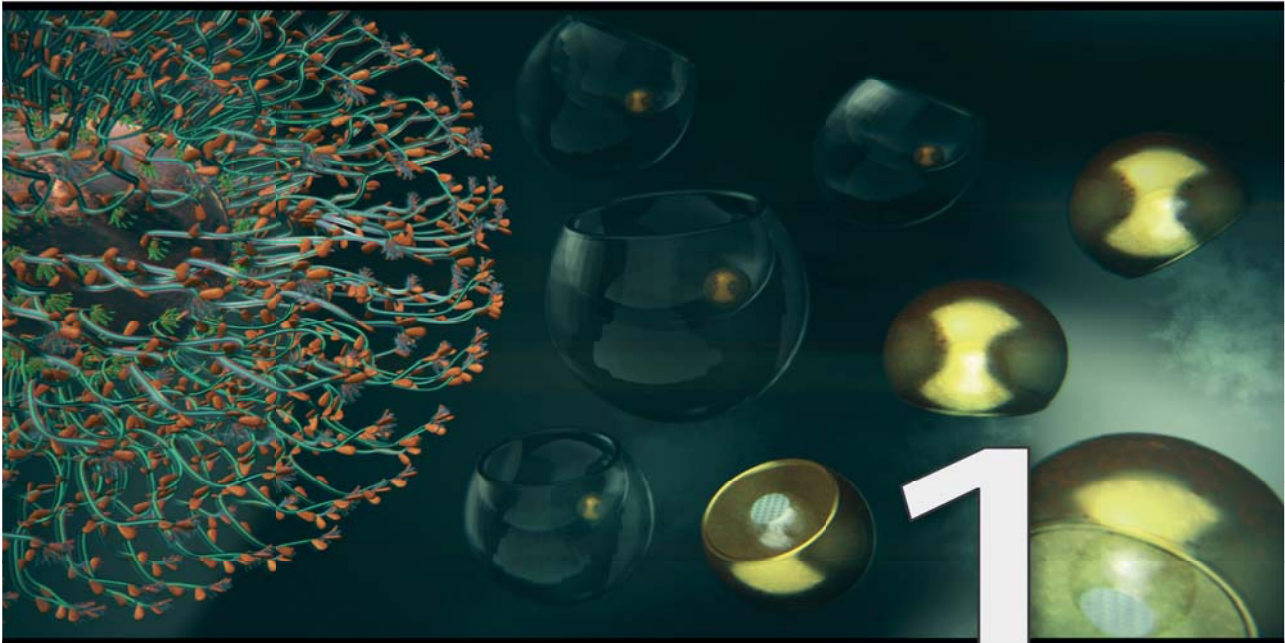


<https://cuvillier.de/de/shop/publications/7809>

Copyright:

Cuvillier Verlag, Inhaberin Annette Jentsch-Cuvillier, Nonnenstieg 8, 37075 Göttingen,  
Germany

Telefon: +49 (0)551 54724-0, E-Mail: [info@cuvillier.de](mailto:info@cuvillier.de), Website: <https://cuvillier.de>



# Introduction

The idea that micro- and nanotechnology might make it possible to “to swallow the surgeon” who performs surgery on a patient without causing harm has been a vision since Richard Feynman’s famous 1959 lecture “There is plenty of room in the bottom”<sup>1</sup>. Being able to build a world of nanometer machines and devices is still a major goal in nanotechnology research. Understanding the properties of materials and systems at this scale is crucial for achieving this goal. Materials at the nanometer scale change their behavior according to shape, structure and composition, which allows the tuning of a nanostructure’s properties, a nanotechnologist’s dream<sup>2</sup>.

When it comes to the design of nanomachines, nature’s self-assembled molecular enzyme motors serve as an inspiration. Held together by molecular interactions, such as hydrogen bonds, the molecular building blocks assemble into large, sophisticated supramolecular structures. Supramolecular chemistry, takes into account the reversible noncovalent interactions between components (molecules, molecular subunits or nanoparticles), and thus can explain key concepts of biological systems, like enzyme-substrate interactions or molecular recognition. Recently, the development of self-assembled mechanically interlocked molecular architectures, where rotaxanes and catenanes are synthesized as molecular switches that move with respect to one

another based on an external input<sup>3,4</sup>; has closed the gap between supramolecular chemistry and nanofabrication. It is interesting to consider if nanoparticles can also be used to perform functions that are associated with the aforementioned rudimentary machines or that might even mimic some of the functions of biological nanomotors. This thesis shows that nanoparticles can be fabricated that i) serve as cages similar to what is known in supramolecular chemistry, and that ii) can actively move by themselves, although with a different mechanism to that of molecular motors.

Both tasks require the nanoparticles to have special “symmetry-broken” shapes. Chemical wet synthesis of nanoparticles is a well-known bottom-up fabrication method for nanostructures, but particles obtained via this method tend to be highly symmetric because of surface energy minimization, thus shape control is difficult to achieve. Controlling the material composition and distribution using wet-synthetic methods is only possible within some range. Scaling down top-down fabrication methods in order to obtain complex-shaped nanoparticles is also challenging. However, combinations of top-down methods like nanolithography and bottom-up strategies like layer-by-layer fabrication or self-assembly are promising for the design of functional nanomaterials, with anisotropic shapes and material composition<sup>2</sup>. The fabrication approach for the nanocolloids used in this thesis also relies on a combined bottom-up / top-down approach. The fabrication has been established in A. Mark et. al.<sup>5</sup>, and it allows for the growth of large numbers of asymmetric nanostructures in a controlled manner at the wafer scale, while offering the possibility of interchanging materials for different functionalities and applications<sup>5</sup>. The method is explained in greater detail in chapter 0, where it is used to grow asymmetric inorganic nanoparticles that possess a ~25 nm cavity. This inorganic nanovessel contains a metallic nanoparticle that mimics an organic host-guest complex. The triggered release of the guest particle is demonstrated<sup>6</sup>. While the aim of this chapter is to show-case the ability to grow complex functional nanostructures, the following chapters examine how nanostructures can be made to self-propel (chapter 0) and to self-assemble and function as a chemical pump (chapter 0).

The challenge to build nanostructures that perform mechanical operations (move to a target or deliver a cargo based on external stimuli), is a topic currently being address by researchers in a

wide range of topics worldwide<sup>7-9</sup>. In the last decades, claims of successful fabrication of manmade micro- and nano- objects as for environmental remediation<sup>10,11</sup>, drug delivery systems<sup>12-15</sup> and assembly of supramolecular structures<sup>16</sup>, among other applications; have been numerous made, but these demonstrations await the transition from a proof-of-concept experiment to the real world<sup>8,17-20</sup>. The nanostructures are called chemical nanomotors, as they are capable of converting energy into movement, which necessarily means that they can swim in fluids at low Reynolds number, or cause fluid flow at low Reynolds number<sup>7,8</sup>. Both are demonstrated in this thesis.

Chapter 0 shows experimental results that demonstrate the smallest artificial nanoparticle-nanomotors fabricated to date<sup>21</sup>. Platinum-gold Janus nanoparticles in hydrogen peroxide solution are used as model nanoswimmers. The disproportionation of hydrogen peroxide at the platinum surface causes the particles to generate a product gradient on their surface and thereby enhanced diffusion by self-propulsion. The increase of the diffusion coefficient of the Janus nanomotors is directly related to the concentration of the hydrogen peroxide in the solution. The tracking for such small objects is challenging. By using a dynamic light scattering and analyzing the apparent size change of the objects while changing the fuel concentration, it was possible to determine the diffusion changes of the nanoparticle nanomotors.

Most of the nanomotors that have been fabricated to date use hydrogen peroxide or similar toxic chemicals as a source of fuel for their self-propulsion. Alternatives to hydrogen peroxide as a fuel have been realized, for example where the catalytic site of the motor is consumed (magnesium chloride in water or zinc in acid solution)<sup>22,23</sup> but since the catalyst is consumed during the reaction the life-time of these motors is severely restricted. It is therefore of interest to develop nanomotors that do not use toxic chemicals, are biocompatible and can operate for longer times. Replacing the inorganic catalyst with enzymes takes advantage of the natural catalytic activity of the enzymes to harvest chemical energy from biocompatible specific fuels. By modifying particles in an asymmetric way, the enzymes will generate the necessary gradient for the particles to show self-diffusiophoresis<sup>24</sup>. Since the turnover in enzymes is typically less than in hydrogen peroxide driven motors, the enzyme-powered motors are generally less efficient. The efficiency should increase if more enzymes are located on the nanoparticle. Based on this premise, M13

bacteriophages are genetically modified, and linked to Janus particles. The bacteriophages provide a large surface area and serve as templates for enzyme coupling. Chapter 0, discusses this hybrid construct consisting of a Janus particle, M13 bacteriophages and enzymes, that functions as an enzyme-powered nanomotor. Rather than tracking the motion of these structures, their activity is observed by their ability to pump fluids. This enzyme-virus-particle construct serves as a pump and allows to demonstrate the highest pumping speeds reported to date.

A theoretical background for the results chapters is found in chapter 1, and conclusions are drawn in chapter 0.

---

The results presented in this thesis have in part been published (or will be published in the near future). In particular, excerpts and figures throughout this Ph.D. thesis were taken from the following sources:

#### **Chapter III:**

- M. Alarcón-Correa, T.-C. Lee and P. Fischer, “Dynamic inclusion complexes of metal nanoparticles inside nanocups”, *Angewandte Chemie Int. Ed. Engl.* 2015, 54(23), 6730.

#### **Chapter IV:**

- M. Alarcón-Correa, D. Walker, T. Qiu and P. Fischer, “C5 Nanomotors”, Lecture notes for the DFG SPP 1726 Summer school, 2015, ISBN 978-3-95806-083-8.
- M. Alarcón-Correa, D. Walker, T. Qiu and P. Fischer, “Nanomotors”, *The European Physical Journal Special Topics*, 2016, 225, 11-12, 2241.
- T.-C. Lee, M. Alarcón-Correa, C. Miksch, K. Hahn, J. G. Gibbs and P. Fischer, “Self-propelling nanomotors in the presence of strong Brownian forces” *Nano Lett.*, 2014, 14, 2407.

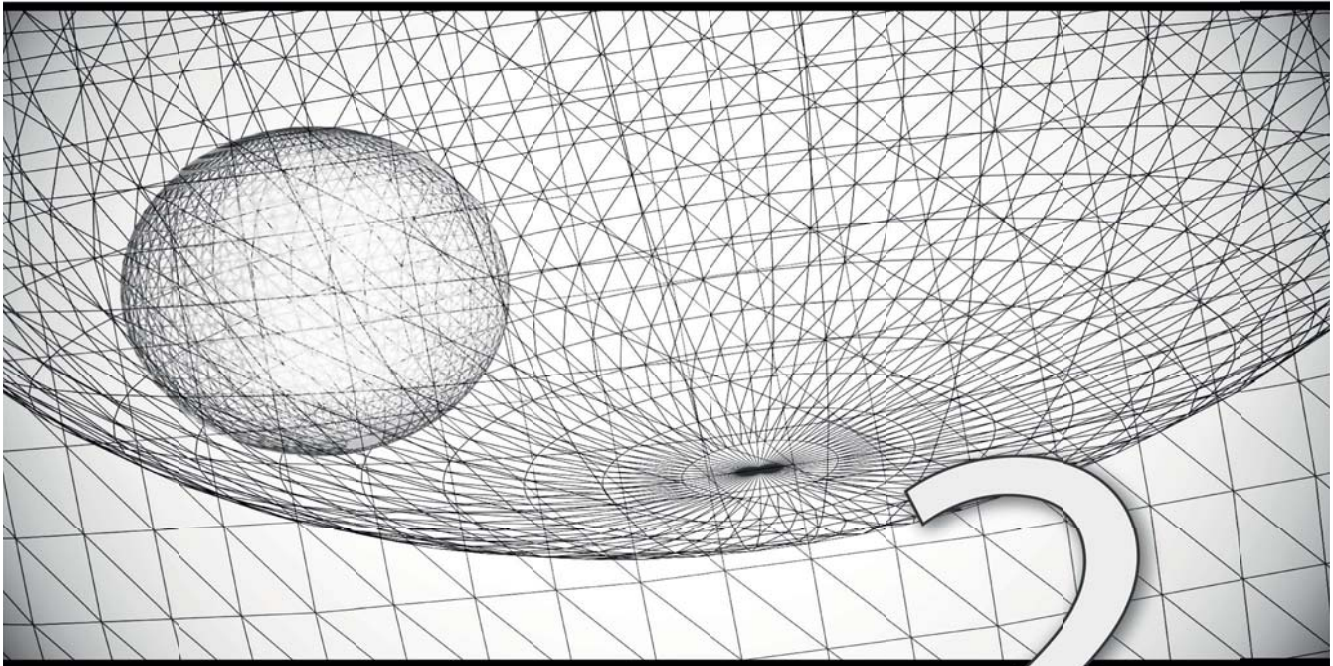
#### **Chapter V:**

- M. Alarcón-Correa, J.-P. Günther, D. Rothenstein, J. Troll, V.M. Kadiri, Bill, P. Fischer, manuscript prepared for submission.

In addition, the author has published the following work during her Ph.D., which is not included in this thesis:

- H.-H. Jeong, M. Alarcón-Correa, A. G. Mark, K. Son, T.-C. Lee and P. Fischer, “Corrosion-Protected Hybrid Nanoparticles”, *Adv. Sci.*, 2017, 1700234.
- H.-H. Jeong, A.G. Mark, M. Alarcón-Correa, I. Kim, P. Oswald, T.-C. Lee and P. Fischer, “Dispersion and shape engineered plasmonic nanosensors”, *Nature Communications*, 2016, 7, 11331.
- H.-H. Jeong, A.G. Mark, T.-C. Lee, M. Alarcón-Correa, S. Eslami, T. Qiu, J.G. Gibbs and P. Fischer, “Active nanorheology with plasmonics”, 2016, *Nano Lett.*, 16, 8, 4887.
- H.-H. Jeong, A.G. Mark, T.-C. Lee, K. Son, W. Chen, M. Alarcón-Correa, I. Kim, G. Schütz, P. and Fischer, “Selectable Nanopattern Arrays for Nanolithographic Imprint and Etch-Mask Applications” 2015, *Adv. Sci.*, 2, 7, 1500016.
- S. Eslami, J.G. Gibbs, Y. Rechkemmer, J. van Slageren, M. Alarcón-Correa, T.-C. Lee, A.G. Mark, G. LJA Rikken and P. Fischer, “Chiral nanomagnets”, 2014, *ACS Photonics*, 1, 12, 1231





# Theoretical Background

## 2

The present chapter is written as an introduction of the general theoretical aspects behind this work. The first part of the chapter discusses propulsion at small length scale, including a brief discussion of Brownian motion, movement at low Reynolds number, and the self-propulsion mechanism of particles.

The inclusion complexes of Chapter 0 are thought to form by a cascade of processes including solid-state diffusion, galvanic corrosion and the Kirkendall effect, which are introduced here.

The description of the bacteriophages and enzymes, components of the biocompatible nanomotors of Chapter 0 make use of chemical reactions, which are collectively discussed in section 2.4.

Finally, the theoretical principles and principle of operation of the most important experimental techniques used in this thesis are also discussed.



## 2.1. Hydrodynamics at low Reynolds number

All of this work is in liquids and concerns small particles. Liquids deform constantly without compressing under shear forces and can, in the continuum approximation, be described without recourse to the molecules that make up the fluid. Considering a fluid volume, then conservation of mass and momentum and assuming there is no dissipation in the fluid, one obtains the following continuity equation

$$\frac{\partial \rho}{\partial t} + \rho \nabla \cdot \vec{v} = 0 \quad (1)$$

A small particle of length  $L$  moving in a fluid with a speed  $U$ , the Reynolds number  $Re = \rho LU / \mu$  corresponds to the ratio between inertial and viscous forces. The density of the fluid is  $\rho$ , its velocity  $v$  and  $\eta$  the viscosity.  $Re$  is about  $10^6$  for a swimming human and  $10^{-4}$  for a bacterial cell<sup>25</sup>. Therefore, colloids are subject to low- $Re$  hydrodynamics, where inertia is negligible compared to the viscous forces. It follows that at low Reynolds number, with  $Re \ll 1$ , the flow of an incompressible Newtonian fluid with density  $\rho$  and dynamic viscosity  $\eta$  is in the absence of any external forces described by the Stokes equations:

$$-\nabla p + \eta \nabla^2 \mathbf{v} = 0, \quad \nabla \cdot \mathbf{v} = 0, \quad (2)$$

which show no explicit time-dependence. It follows that it is not possible to swim with a time-reversible motion or flow. This is also known as the scallop theorem.<sup>25</sup> If the colloids are to swim, then they must break symmetry in the flows they generate. This is achieved by the Janus structure. The Janus colloids must first form a stable colloidal dispersion.

### 2.1.1 Colloidal solutions

A colloidal dispersion is a stabilized two-phase system: colloids in a dispersion medium, here the fluid. The colloidal particles of chapters 3 and 4 are inorganic particles and the assumption of hard spheres that is generally made applies. The colloids are immersed in a continuum (one-component model) fluid and the forces acting between the hard spheres are generally described by the **DLVO** (Derjaguin, Landau, Verwey, and Overbeek) theory<sup>26,27</sup>. This theory describes the stability of the dispersions as the balance of two types of interactions between the colloids a distance  $d$  apart: electrostatic repulsion ( $W(d)_R$ ) and some attractive interaction (generally van der Waals forces) ( $W(d)_A$ )<sup>28,29</sup>:

$$W(d) = W(d)_A + W(d)_R \quad (3)$$

While the dispersion is overall electrically neutral, the charges near a colloid are not homogeneously distributed. A particle in solution will usually carry an effective surface charge and an excess of counter-ions will form a relatively strongly bound layer around the immediate surface of the particle (Stern layer). For instance, a negatively charged particle will attract positive counter ions. A second (diffuse) layer of more loosely bound negative and positive charged ions surrounds the Stern layer. This second layer extends to a so-called “slipping plane”, outside of which charges are isotropically organized and homogeneously distributed (Figure 1).

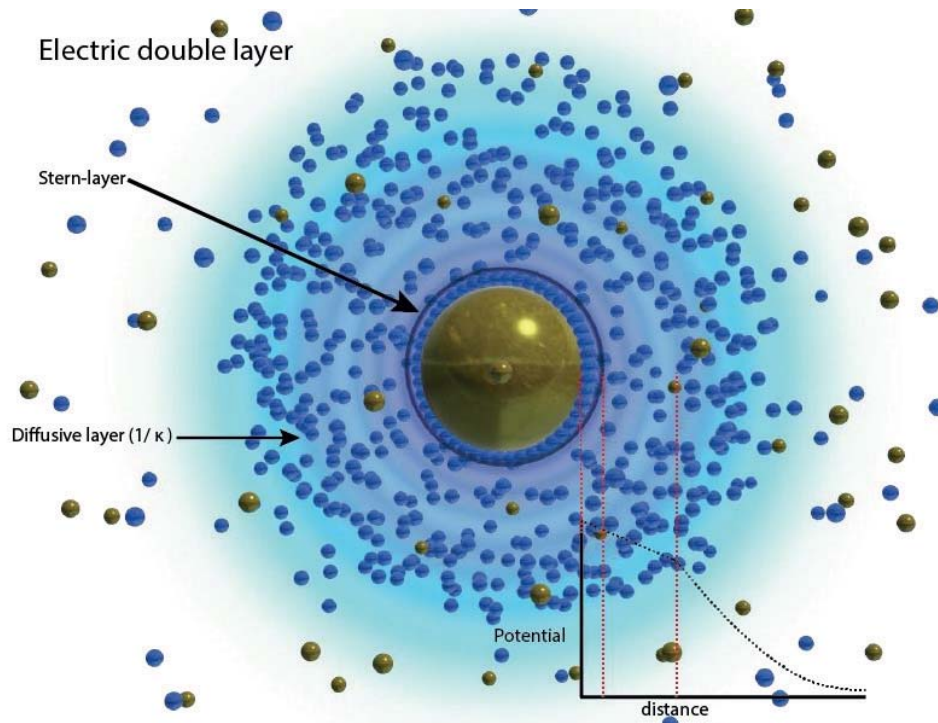


Figure 1. Double layer model. The effective charge of the colloidal particle will electrostatically attract ions in solution of opposite charge. These strongly attached ions will form a layer known as the Stern layer, followed by a diffusive layer, where the charge of the colloid will still attract counter ions, but the Stern layer will repel them. The effective charge is screened until both positive and negative ions in solution are again equally distributed. Based on Ref.<sup>28</sup>

This double-layer causes a charge gradient around the particle with a higher charge density closest to the particle, decreasing with distance. To illustrate the interaction forces of two particles, the interactions between two half planes are usually considered. The long-ranged electrostatic repulsion force is of a form:

$$W(d)_R = \frac{64kTc\Gamma_0^2 e^{-\kappa d}}{\kappa}, \quad (4)$$

where  $c$  represents the electrolyte concentration in the bulk,  $d$  = distance between colloids,  $\kappa$  = reciprocal Debye-Hückel screening length, and  $\Gamma_0$  is related to the contribution of overlapping double layers and the surface potential of the interacting particles.

This repulsion is countered by an van der Waals attraction<sup>30</sup>:

$$W(d)_A = -\frac{H}{12\pi d^2} \quad (5)$$

Where  $H$  (Hamaker constant) is material-dependent. In most cases,  $H$  is positive, yielding an attractive potential.

The combination of these two forces, gives a separation-dependent net energy, that explains why colloids aggregate or not. (Figure 2). Since the size of the double layer depends on the solution in which the colloidal particles are found, the concentration of ions, pH changes, salt additions, etc., determines the stability of the colloid dispersion. Particles aggregation, precipitation, and flocculation can be induced by changes in the solution; the repulsive forces can be increased in a way that the colloids do not aggregate. In the same way, the stability can be affected if some materials are added to the surface of the colloidal particles, changing the van der Waals attraction potential of the particles<sup>28</sup>.

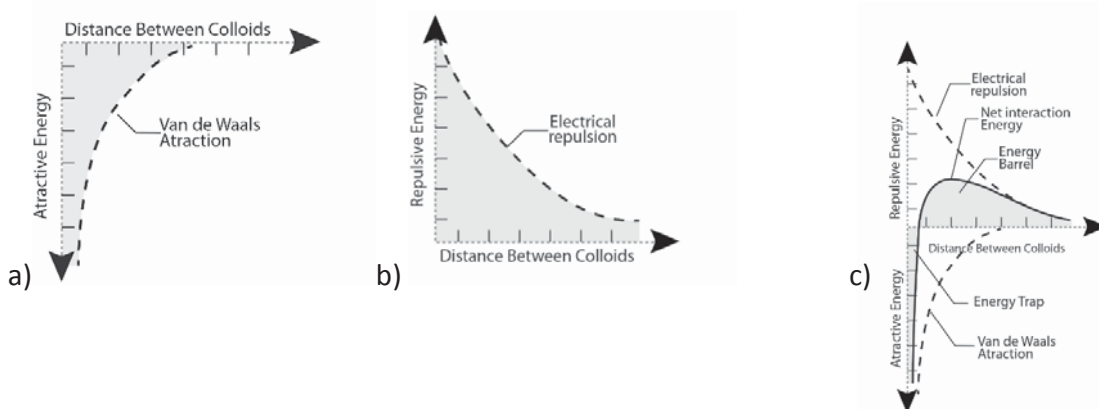


Figure 2. DVLO Theory. The net interaction of the colloids is given by the black curve in Figure 2 c. it is formed by combining the attraction curve of the van der Waals interactions (Figure 2a) with the electrostatic repulsion curve (Figure 2b). Based on Ref.<sup>28</sup>